Behavioral/Cognitive

# A Conditioned Place Preference for Heroin Is Signaled by Increased Dopamine and Direct Pathway Activity and Decreased Indirect Pathway Activity in the Nucleus Accumbens

**Timothy J. O'Neal,**[1,2,3,4] **Mollie X. Bernstein,**[1] **Derek J. MacDougall,**[3] **and Susan M. Ferguson**[2,3,4]

[1]Graduate Program in Neuroscience, University of Washington, Seattle, Washington 98195, [2]Department of Psychiatry & Behavioral Sciences, University of Washington, Seattle, Washington 98195, [3]Center for Integrative Brain Research, Seattle Children's Research Institute, Seattle, Washington 98101, and [4]Addictions, Drug & Alcohol Institute, University of Washington, Seattle, Washington 98195

**Repeated pairing of a drug with a neutral stimulus, such as a cue or context, leads to the attribution of the drug's reinforcing properties to that stimulus, and exposure to that stimulus in the absence of the drug can elicit drug-seeking. A principal role for the NAc in the response to drug-associated stimuli has been well documented. Direct and indirect pathway medium spiny neurons (dMSNs and iMSNs) have been shown to bidirectionally regulate cue-induced heroin-seeking in rats expressing addiction-like phenotypes, and a shift in NAc activity toward the direct pathway has been shown in mice following cocaine conditioned place preference (CPP). However, how NAc signaling guides heroin CPP, and whether heroin alters the balance of signaling between dMSNs and iMSNs, remains unknown. Moreover, the role of NAc dopamine signaling in heroin reinforcement is unclear. Here, we integrate fiber photometry for *in vivo* monitoring of dopamine and dMSN/iMSN calcium activity with a heroin CPP procedure in rats to begin to address these questions. We identify a sensitization-like response to heroin in the NAc, with prominent iMSN activity during initial heroin exposure and prominent dMSN activity following repeated heroin exposure. We demonstrate a ramp in dopamine activity, dMSN activation, and iMSN inactivation preceding entry into a heroin-paired context, and a decrease in dopamine activity, dMSN inactivation, and iMSN activation preceding exit from a heroin-paired context. Finally, we show that buprenorphine is sufficient to prevent the development of heroin CPP and reduce Fos activation in the NAc after conditioning. Together, these data support the hypothesis that an imbalance in NAc activity contributes to the development of drug-cue associations that can drive addiction processes.**

*Key words:* **dopamine; fiber photometry; heroin; NAc; reward**

### Significance Statement

**The attribution of the reinforcing effects of drugs to neutral stimuli (e.g., cues and contexts) contributes to the long-standing nature of addiction, as re-exposure to drug-associated stimuli can reinstate drug-seeking and -taking even after long periods of abstinence. The NAc has an established role in encoding the value of drug-associated stimuli, and dopamine release into the NAc is known to modulate the reinforcing effects of drugs, including heroin. Using fiber photometry, we show that entering a heroin-paired context is driven by dopamine signaling and NAc direct pathway activation, whereas exiting a heroin-paired context is driven by NAc indirect pathway activation. This study provides further insight into the role of NAc microcircuitry in encoding the reinforcing properties of heroin.**

Received July 14, 2021; revised Dec. 20, 2021; accepted Dec. 23, 2021.

Author contributions: T.J.O. and S.M.F. designed research; T.J.O., M.X.B., and D.J.M. performed research; T.J.O., M.X.B., and D.J.M. analyzed data; T.J.O. wrote the first draft of the paper; T.J.O., M.X.B., D.J.M., and S.M.F. edited the paper; T.J.O. and S.M.F. wrote the paper.

This work was supported by National Institute on Drug Abuse Grant F31DA047012 to T.J.O. and Grant R01DA036582 to S.M.F.; and University of Washington Addictions, Drug & Alcohol Institute ADAI-0138 to T.J.O. We thank Dr. John Neumaier and Dr. Michelle Kelly for providing the CAV2-Cre virus; University of Washington Molecular Genetics Resource Core P30DA048736 for producing the AAV1-dLight1.3b virus; and Dr. Elizabeth Crummy, Dr. Scott Ng-Evans, and Joshua O'Neal for programming assistance.

The authors declare no competing financial interests.

Correspondence should be addressed to Susan M. Ferguson at smfergus@uw.edu.

https://doi.org/10.1523/JNEUROSCI.1451-21.2021



## Introduction

The opioid epidemic remains a major public health crisis in the United States, with relapse rates and overdose-related fatalities continuing to rise (Hedegaard et al., 2018). One critical mechanism underlying persistent drug-craving is the attribution of the reinforcing properties of a drug to a previously neutral stimulus (conditioned stimulus [CS]; e.g., cues, contexts) (Everitt et al., 2018). Re-exposure to a drug-paired CS can reinstate drug-seeking following action/outcome devaluation (Shaham et al., 2003) or prolonged abstinence (Grimm et al., 2001). The NAc integrates cortical and subcortical inputs to guide behavioral processes

associated with addiction, including associative learning, decision-making, and motivation (Gerfen and Surmeier, 2011; Calabresi et al., 2014; Koob and Volkow, 2016). However, the NAc is heterogeneous, and predominantly comprised of two interspersed populations of medium spiny neurons (MSNs): direct pathway MSNs (dMSNs) that project to the VTA and primarily express the dopamine (DA) D1 receptor, and indirect pathway MSNs (iMSNs) that project to the ventral pallidum (VP) and primarily express the DA D2 receptor. Although dMSNs and iMSNs have canonically been thought to have direct, opposing control over behavior, with dMSNs serving as a "Go" signal to promote action and iMSNs serving as a "Stop" signal to suppress action (Lobo et al., 2010; Ferguson et al., 2011), recent evidence supports a more graded model. For example, mice will seek optogenetic self-stimulation of either dMSNs or iMSNs (Cole et al., 2018); and while brief optogenetic stimulation of either cell type increases the motivation for sucrose, promotes positive reinforcement, and enhances preference for a cocaine-paired context (Soares-Cunha et al., 2016, 2019), prolonged optogenetic stimulation of either cell type promotes aversion (Soares-Cunha et al., 2019). Moreover, chemogenetic inhibition of iMSNs increases the motivation for cocaine but not heroin (Bock et al., 2013; O'Neal et al., 2020), and chemogenetic modulation of dMSNs or iMSNs bidirectionally alters cue-induced heroin-seeking selectively in rats expressing an addiction-like phenotype (O'Neal et al., 2020). Together, these data suggest a nuanced role for NAc dMSNs and iMSNs in behavioral control and highlight the need to investigate these neuronal populations in the context of understudied areas, including opioid addiction.

Midbrain DA release into the NAc is central to the rewarding effects of illicit drugs (Crummy et al., 2020), and phasic DA release into the NAc promotes drug-seeking (Phillips et al., 2003). In addition to slower modulation of dMSNs and iMSNs via activation of G-protein coupled D1 and D2 receptors, DA can rapidly modulate these neuronal populations via opening of $IP_3$ receptors and release of intracellular $Ca^{2+}$ (Swapna et al., 2016), a process that is integral for the propagation of $Ca^{2+}$ waves and heterosynaptic plasticity in the NAc (Bailey et al., 2000; Plotkin et al., 2013). *In vivo* imaging of dMSN and iMSN $Ca^{2+}$ activity has revealed a rapid increase in dMSN activity and a progressive decrease in iMSN activity after acute cocaine exposure (Luo et al., 2011), as well as a persistent attenuation of iMSN activity after chronic cocaine treatment (Park et al., 2013), all of which lead to a long-lasting predominance of dMSN over iMSN signaling. Moreover, a ramping of dMSN $Ca^{2+}$ activity along with a concomitant decrease in iMSN activity has been observed in mice preceding entry into a context associated with cocaine treatment (Calipari et al., 2016). Importantly, psychostimulants and opioids have different mechanisms of action and engage nonoverlapping subcircuits to promote addictive behaviors (Badiani et al., 2011; Crummy et al., 2020), so the temporal relationship between NAc signaling and heroin-seeking cannot necessarily be inferred from cocaine studies.

Recently, we showed that targeted manipulation of NAc dMSNs and iMSNs has oppositional control over cue-induced reinstatement of heroin-seeking but not the motivation to take heroin (O'Neal et al., 2020); however, it remains to be determined how the acquisition of a heroin CS is encoded by signaling in the NAc. Thus, we combined fiber photometry for *in vivo* monitoring of NAc DA signaling and dMSN/iMSN $Ca^{2+}$ signaling with a heroin conditioned place preference (CPP) procedure. NAc activity was recorded during early and late conditioning sessions to assess changes in the neural response over the course of conditioning. Following conditioning, we examined temporally precise DA signaling and activity of dMSNs and iMSNs during entries to and exits from contexts that had been paired with either saline or heroin and compared these signals with those recorded before conditioning. Finally, we explored the effects of buprenorphine, a partial $\mu$ opioid receptor agonist used in opioid-replacement therapy, on the acquisition of heroin CPP and subsequent activation of the NAc.

## Materials and Methods

### *Subjects*

Outbred female ($n = 40$; ~8 weeks old, 175-199 g at arrival; Envigo) and male ($n = 40$; ~8 weeks old, 250-274 g at arrival; Envigo) Sprague Dawley rats were pair-housed in a humidity- and temperature-controlled vivarium, with *ad libitum* access to food and water throughout the experiments. Rats were acclimated to the vivarium for at least 5 d and handled for at least 3 d before any procedures. All procedures were done in accordance with the National Institutes of Health's Office of Laboratory Animal Welfare and were approved by the Seattle Children's Research Institute's Institutional Animal Care and Use Committee.

### *Drugs*

Diamorphine HCl (heroin) was obtained through the Drug Supply Program of National Institute on Drug Abuse and was dissolved in sterile saline (0.9%) to a concentration of 1-3 mg/ml and administered at a dose of 1 ml/kg. Buprenorphine was also obtained through the Drug Supply Program of National Institute on Drug Abuse and was dissolved in sterile saline (0.9%) to a concentration of 0.2 mg/ml and administered at a dose of 1 ml/kg.

### *Viral vectors*

Adeno-associated viruses containing Flp recombinase (AAVrg-EF1$\alpha$-flpo; #55637-AAVrg), Flp-dependent GCaMP6s (AAV8-EF1$\alpha$ -fDIO-GCaMP6s; #105714-AAV8), and Cre-dependent RCaMP1b (AAV1-Syn-FLEX-NES-jRCaMP1b-WPRE-SV40; #100850-AAV1) were acquired from Addgene and had titers of $\geq 1 \times 10^{13}$ viral genomes/ml. dLight1.3b plasmid (AAV1-Syn-dLight1.3b) was acquired from Addgene (#135762) and prepared by the University of Washington's Molecular Genetics Resource Core. Canine adenovirus containing Cre recombinase (CAV2-Cre) had a titer of $\sim 2.5 \times 10^9$ viral genomes/µl and was prepared as previously described (Kremer et al., 2000).

### *Stereotaxic surgery*

Rats were anesthetized with isoflurane (3% induction, 1%-2% maintenance; Patterson Veterinary) and injected with meloxicam (1 mg/ml, 1 ml/kg, s.c.; Patterson Veterinary) for analgesia. Following head-fixation in a digital stereotax (Kopf Instruments), the skull was exposed and scored, and craniotomies were drilled above target nuclei. Viral vectors were loaded into 10 µl gas-tight syringes (Hamilton) and infused unilaterally into target nuclei (500 nl per virus, 100 nl/min). Coordinates (in mm, relative to bregma) (Paxinos et al., 1980) were as follows: NAc (AP 1.5, ML 1.0, DV −7.5), VP (AP 0.2, ML 2.0, DV −8.0), VTA (AP −5.3, ML 0.8, DV −8.3). To target dMSNs, AAVrg-EF1$\alpha$-flpo was infused into the VTA and AAV8-EF1$\alpha$-fDIO-GCaMP6s was infused into the NAc. To target iMSNs, CAV2-Cre was infused into the VP and AAV1-Syn-FLEX-NES-jRCaMP1b-WPRE-SV40 was infused into the NAc. Syringes were left in place for an additional 5 min following infusion and slowly retracted to allow proper diffusion of virus into target nuclei. Following viral infusion, fiber optic cannula (MFC_400/430-0.37_8mm_ZF2.5_FLT; >85% transmittance; Doric Lenses) were implanted in the NAc medial shell (DV −7.4) and secured with skull screws, metabond (Patterson Dental), and dental cement.

### *Fiber photometry*

Three weeks after surgery, fiber photometry recordings were performed using a multiplex photometry system (FP3001; Neurophotometrics). Rats were acclimated to branching fiber optic patch cords (BFP4_400/440/LWMJ-0.37_3m_SMA*-4xFC; Doric Lenses) for at least 3 d before

testing, and biosensor expression was confirmed the day before testing via brief (~5 min) home cage recordings. For all recordings, LEDs were heated at 100% power for at least 5 min before recording to minimize heat-induced LED decay during recordings, then reduced to <50 μW for the duration of recordings (415 and 470 nm: ~12.5 μW; 560 nm: ~25 μW). Photometry recordings with a single biosensor (dLight1.3b imaging) used 2-phase cycling of 415 and 470 nm LEDs (50 ms per channel), and recordings with two biosensors (dual GCaMP6s/RCaMP1b imaging) used 3-phase cycling of 415, 470, and 560 nm LEDs (75 ms per channel). Fluorescent signals were bandpass filtered, collimated, reflected by a dichroic mirror, and focused by a 20× objective (0.40 NA) on the sensor of a CMOS camera. Signals were collected via custom-written workflows in Bonsai and exported for offline analysis via open-source and custom-written Python scripts.

### CPP

*CPP apparatus.* Behavioral sessions were conducted in custom-built acrylic chambers (TAP Plastics) with two equally sized but visually distinct chambers (15 in. wide × 15 in. long × 12 in. tall), and a smaller center chamber (6 in. wide × 15 in. long × 12 in. tall) separated from the outer chambers via removable guillotine doors (3 in. wide × 12 in. tall). The walls of the two outer chambers were covered with visually distinct wallpapers (honeycomb and zebra, both grayscale), and the floor of the entire apparatus was matte black to facilitate behavioral tracking. USB cameras (2.1 mm, wide-angle; ELP) were positioned above CPP chambers and interfaced with Bonsai for motion tracking. Video streams were grayscaled and thresholded, and binary region analysis was used to detect animal position within the CPP chambers. Chambers were cleaned between sessions with 70% ethanol (w/v).

*CPP procedure.* Experimental parameters were chosen based on a meta-analysis of heroin CPP by Bardo et al. (1995) to maximize potential effect sizes. The overall CPP procedure included an initial preference test (15 min, beginning at 11:00), eight conditioning sessions (2×/day, 40 min each), and a final preference test (15 min, beginning at 11:00). During the preference tests, the guillotine doors were removed, and subjects were placed in the center of the neutral chamber and allowed to freely explore the full apparatus. During conditioning sessions, subjects received intraperitoneal injections of saline (09:00) or heroin (13:00) and were immediately confined to one of the outer chambers. Side pairings were assigned in a pseudorandomized, counterbalanced design to avoid sex or treatment biases with either chamber. Pretreatment injections of buprenorphine were given 10 min before injections of saline or heroin. All behavioral testing was done during the light cycle because of the use of visual cues for conditioning.

### Immunohistochemistry

After behavioral testing, rats were deeply anesthetized with Euthasol (2 ml/kg i.p.; 3.9 mg/ml pentobarbital sodium and 0.5 mg/ml phenytoin sodium; Patterson Veterinary) and transcardially perfused with PBS, pH 7.4, followed by PFA (4% in PBS). Brains were extracted, fixed overnight in 4% PFA, postfixed for >48 h in sucrose (30% in PBS), and sectioned (50 μm) with a vibrating microtome. Floating sections were washed (PBS; 3 × 10 min), blocked (0.25% Triton-X, 5% normal goat serum, PBS; 2 h), and incubated with primary antibodies (0.25% Triton-X, 2.5% normal goat serum, PBS; 24 h) against Fos (1:800 rabbit anti-cFos, Cell Signaling, #2250; RRID:AB_2247211) or TH (1:400 mouse anti-TH, Sigma, #MAB318; RRID:AB_2201528). Sections were then washed (PBS; 3 × 10 min) and incubated with secondary antibodies (0.25% Triton-X, 2.5% normal goat serum, PBS; 2 h) conjugated to AF-568 (1:500 goat-anti-rabbit, Invitrogen, #A11011; RRID:AB_143157) or AF-647 (1:500 goat-anti-mouse, Invitrogen, #A21236; RRID:AB_2535805). Finally, sections were washed (PBS; 3 × 10 min), mounted on slides, and coverslipped with mounting medium with DAPI (Vectashield). *Z* stacks along the rostral-caudal axis of the NAc (AP 2.5 through AP 0.7) were collected with confocal microscopy (20×; Carl Zeiss LSM 710), and $Fos^+$ cells were quantified using ImageJ (version 1.49; National Institutes of Health).

### Experimental design and statistical analyses

Behavioral and photometry data were collected using custom-written workflows (Bonsai version 3.5.2), processed using custom-written and open-source Python scripts (version 3.7.7), analyzed using Python and GraphPad Prism (version 9.0), and visualized with GraphPad Prism and Adobe Illustrator (CC 2020). Transitions between chambers and cumulative time spent in each chamber were detected via binary region analysis in Bonsai and analyzed in Python. Heroin preference was calculated as the difference in time spent between chambers (i.e., Heroin preference = [time in heroin-paired] − [time in saline-paired]), and final preference was calculated as the change in preference across test sessions (i.e., CPP score = [Heroin preference, postconditioning] − [Heroin preference, preconditioning]). Change in preference was analyzed using two-way repeated-measures ANOVA (dose × test) or two-tailed paired *t* tests, and final preference was analyzed using one-way ANOVA. Equal numbers of female and male rats were included in each experiment, and sex differences in final preference were analyzed using two-way ANOVA (sex × dose) or two-tailed unpaired *t* tests. $Fos^+$ cell counts along the rostral-caudal axis of the NAc were averaged into a single value per rat and analyzed using two-tailed unpaired *t* tests for each subregion. Photometry signals were analyzed as described by Martianova et al. (2019) (code available at: www.github.com/katemartian/Photometry_data_processing). Raw photometry signals were de-interleaved to isolate reference (415 nm) and experimental (470 nm, 560 nm) signals, and a moving average (window size = 1.5s [dLight: 20 data points; GCaMP/RCaMP: 30 data points) was applied to remove high-frequency artifacts from each signal. Next, adaptive iteratively reweighted Penalized Least Squares was applied to each signal, and the resulting baseline was subtracted to correct for photobleaching. Reference and experimental signals were then independently normalized to *z* scores ($F_n - F_{mean}/F_{SD}$, where $F_{mean}$ and $F_{SD}$ are the mean/SD from the entire recording session for each channel), and the resulting *z*-scored reference signal was regressed onto and subtracted from the *z*-scored experimental signals to yield normalized experimental signals (zdFF). Events were detected in zdFF signals collected during conditioning sessions by identifying peaks (i.e., $zdFF_n > zdFF_{n-1}$ and $zdFF_{n+1}$) where $z > 2.58$ ($p < 0.01$), using the detect_peaks Python function developed by Duarte and Watanabe (2021) (code available at: www.github.com/demotu/BMC). To check for residual motion artifacts in normalized signals, instantaneous speed was extracted from behavioral tracking data, and linear regressions were performed between speed and photometry. To check for independence between GCaMP6s and RCaMP1b signals, linear regressions and cross-correlations were performed between signals. Photometry signals during conditioning sessions were processed (event frequency, mean amplitude, variance of amplitudes) and analyzed using two-way repeated-measures ANOVA (session × drug) and Kolmogorov–Smirnov tests (cumulative distribution of amplitudes). Photometry signals during test sessions were aligned to transitions between chambers, and the window centered around each transition (−3 to 3 s) was extracted for analysis. Given individual variability in the number of transitions made during test sessions (pre: 9.1 ± 0.6, range = 5-18; post: 13.7 ± 0.92, range = 7-31), analysis was limited to the first five transitions of each type. Mean signals at transition (zdFF at time = 0 s) were analyzed using two-way repeated-measures ANOVA (chamber × test), and cumulative signals during the transition window (area under the curve) were calculated using trapezoidal numerical integration and analyzed using two-way repeated-measures ANOVA (chamber × test). Statistical significance for all analyses was set at $p < 0.05$, and all ANOVAs were followed by Sidak *post hoc* tests (behavioral data) or Benjamini and Hochberg FDR tests with $q < 0.05$ (photometry data). Data are shown throughout as individual subjects and/or mean ± SEM. Subjects with lack of viral expression ($n = 10$), incorrect fiber placement ($n = 4$), or no change in preference for the heroin-paired chamber (CPP score < 0; $n = 5$) were excluded from fiber photometry experiments.

## Results

### Expression of heroin CPP is accompanied by robust activation of the NAc

Female and male rats underwent a heroin CPP procedure that included an initial chamber preference test, 4 d of conditioning,

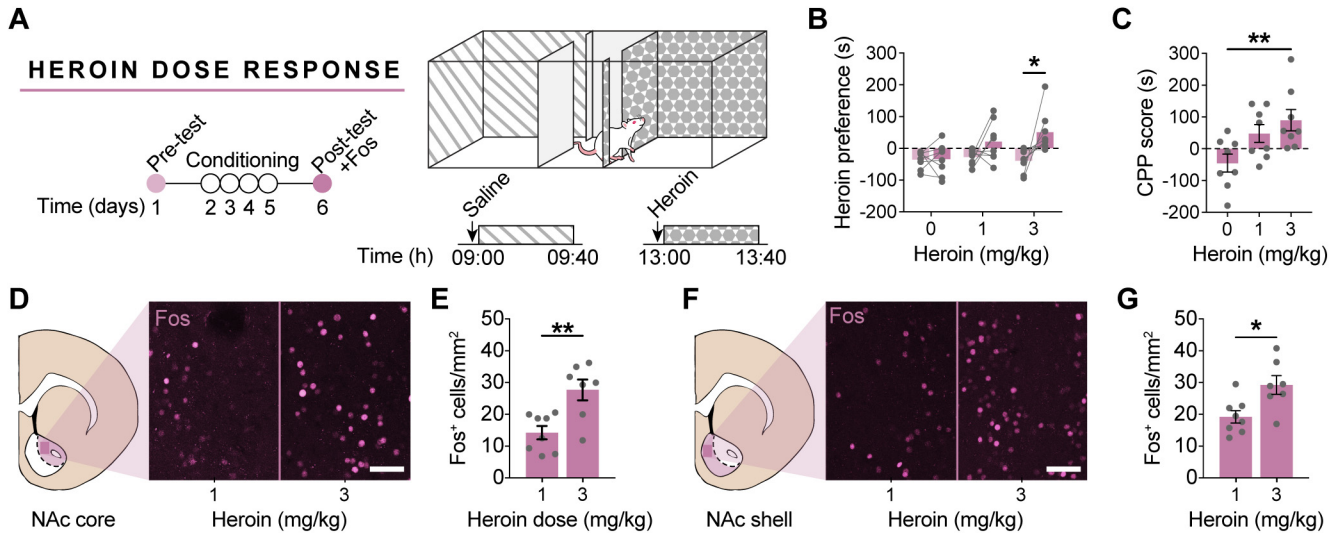


**Figure 1.** Expression of heroin CPP is accompanied with NAc activation. ***A***, Timeline for heroin CPP procedure. Rats underwent two preference tests (15 min each) separated by eight conditioning sessions (2×/day, 40 min each), and activation of the NAc during the post-test was assessed via Fos immunohistochemistry. ***B***, ***C***, Rats conditioned with 3 mg/kg heroin spent more time in the heroin-paired chamber during the post-test and developed a significant preference for the heroin-paired chamber. ***D–G***, Representative images and quantification of Fos in the NAc. Rats conditioned with 3 mg/kg heroin had significantly more Fos in the NAc core and shell during the post-test than those conditioned with 1 mg/kg heroin. $n = 8$/group. Scale bar, 50 µm. $^*p < 0.05$. $^{**}p < 0.01$.

and a final chamber preference test (Fig. 1*A*). To identify a dose of heroin that would reliably produce a CPP, rats were conditioned with 0, 1, or 3 mg/kg heroin. A two-way repeated-measures ANOVA revealed a significant dose × test interaction on preference for the heroin-paired chamber ($F_{(2,21)} = 5.40$, $p = 0.013$), with rats conditioned with 3 mg/kg heroin significantly increasing time spent in the heroin-paired chamber in the post-test compared with the pretest ($p = 0.023$; Fig. 1*B*). Moreover, a one-way ANOVA revealed a significant main effect of dose on final preference ($F_{(2,21)} = 5.28$, $p = 0.014$), with rats conditioned with 3 mg/kg heroin ($p = 0.0091$) but not 1 mg/kg heroin ($p = 0.078$) developing a stronger CPP for the heroin-paired chamber than rats conditioned with 0 mg/kg heroin (Fig. 1*C*). To assess the role of the NAc in expression of a heroin CPP, rats were killed 30 min after the final preference test, and brains were processed for Fos immunohistochemistry. An unpaired *t* test revealed a significant effect of dose on Fos activation in the NAc core ($t_{(13)} = 3.54$, $p = 0.0036$), with significantly greater activation in rats conditioned with 3 mg/kg heroin (Fig. 1*D*,*E*). Similarly, an unpaired *t* test revealed a significant effect of dose on Fos activation in the NAc shell ($t_{(13)} = 2.94$, $p = 0.012$), with significantly greater activation in rats conditioned with 3 mg/kg heroin (Fig. 1*F*,*G*). Of note, two-way ANOVAs revealed no main effect of sex on final preference for the heroin-paired chamber ($F_{(1,18)} = 2.46$, $p = 0.13$) or Fos activation in the NAc core ($F_{(1,11)} = 0.0032$, $p = 0.96$) or NAc shell ($F_{(1,11)} = 2.17$, $p = 0.17$), so male and female data were combined for all subsequent analyses.

### *In vivo* imaging of DA activity and MSN calcium activity in the NAc

To examine the role of NAc activity in the development and expression of a heroin CPP with temporal precision, CPP was coupled with fiber photometry for *in vivo* monitoring of DA signals, dMSN $Ca^{2+}$ signals, and iMSN $Ca^{2+}$ signals. Photometry signal quality was verified before starting CPP via brief home cage recordings from pairs of rats (Fig. 2*A*). Recordings were performed using either 2-channel imaging for DA photometry or 3-channel imaging for simultaneous dMSN/iMSN photometry, with the reference channel interleaved with experimental channels to correct for motion artifacts and photobleaching (Fig. 2*B*). DA imaging was performed with the DA sensor dLight1.3b (Patriarchi et al., 2018), a modified D1-type DA receptor with a cpGFP insert that expresses proximally to $TH^+$ DA terminals in the NAc (Fig. 2*C–E*). Dual dMSN/iMSN $Ca^{2+}$ imaging was performed with the green-shifted and red-shifted $Ca^{2+}$ indicators GCaMP6s and RCaMP1b, respectively, which were selectively targeted to dMSNs and iMSNs by infusing retrogradely transported recombinases into the VTA (AAVrg-flpo to target dMSNs) and VP (CAV2-Cre to target iMSNs; Fig. 2*F*). GCaMP6s and RCaMP1b expression was detected throughout the NAc, with limited coexpression along the rostral-caudal axis (Fig. 2*G*,*H*). While most rats coexpressed both indicators in the NAc ($n = 8$), a minority exclusively expressed GCaMP6s ($n = 4$) or RCaMP1b ($n = 2$); thus, for all MSN $Ca^{2+}$ imaging experiments, GCaMP6s and RCaMP1b signals were independently analyzed. To confirm that fluctuations in normalized signals were biologically relevant and did not simply reflect motion artifacts, photometry signals were regressed onto instantaneous speed recorded during the pretest. Linear regression found no significant correlation between speed and dLight1.3b (*r*, range: −0.043 to 0.078; $p > 0.15$), GCaMP6s (*r*, range: −0.056 to 0.035; $p > 0.13$), or RCaMP1b (*r*, range: −0.043 to 0.056; $p > 0.20$) signals (Fig. 2*I*). To confirm independence of normalized GCaMP6s and RCaMP1b signals, GCaMP6s signals were regressed onto RCaMP1b signals recorded during the pretest, and the maximally correlated time-shift and corresponding correlation coefficient were calculated. Linear regression found no significant correlation between GCaMP6s and RCaMP1b signals (*r*, range: −0.0004 to 0.19; $p > 0.11$; Fig. 2*J*), and cross-correlation found no relationship between signals, with a negative time-shift (i.e., peak correlation when RCaMP1b precedes GCaMP6s) and a positive time-shift (i.e., peak correlation when GCaMP6s precedes RCaMP1b) in equal numbers of rats ($n = 4$ each).

### Heroin conditioning increases the frequency of NAc DA signaling

After confirming the quality of photometry signals, rats underwent heroin CPP with a conditioning dose of 3 mg/kg. NAc DA signals were recorded at four time points during conditioning:

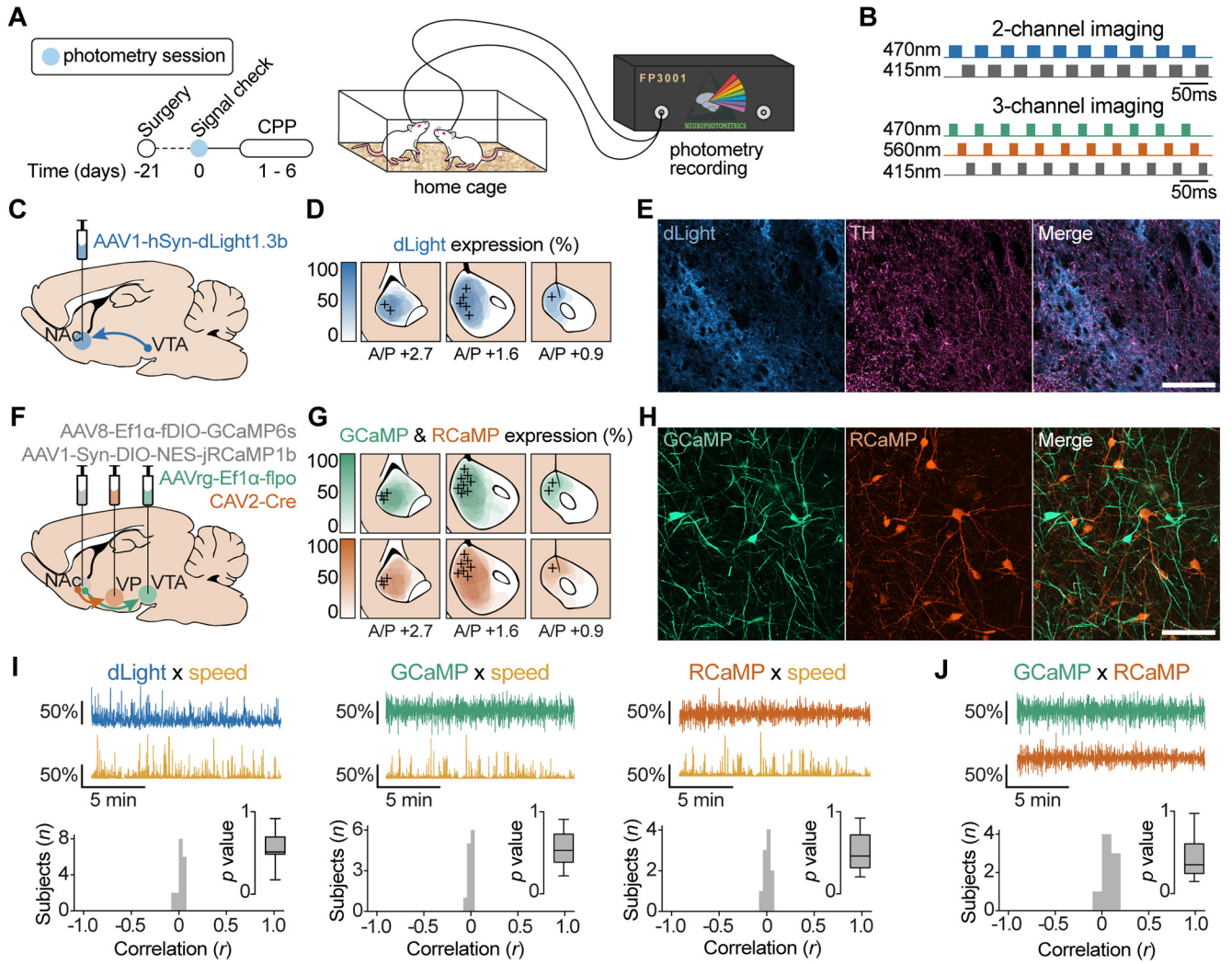


**Figure 2.** Experimental design for fiber photometry recordings in the NAc. ***A***, Timeline for photometry recordings before CPP. Rats underwent brief (~5 min) recordings in their home cages to verify signal quality. ***B***, LED configuration for single- or dual-color imaging with interleaved reference channel. ***C***, ***D***, Viral strategy for DA imaging and expression of dLight1.3b throughout the NAc. ***E***, Representative dLight1.3b expression with TH staining of DA terminals in the NAc. ***F***, ***G***, Viral strategy for dMSN/iMSN $Ca^{2+}$ imaging and expression of GCaMP6s and RCaMP1b throughout the NAc. ***H***, Representative GCaMP6s and RCaMP1b expression in the NAc. ***I***, Photometry signals do not correlate with movement. Top, Representative photometry and speed traces. Bottom, Distribution of correlation coefficients and corresponding *p* values. ***J***, GCaMP6s and RCaMP1b signals are not correlated. Top, Representative traces. Bottom, Distribution of correlation coefficients and corresponding *p* values. +, Optic fiber location. Scale bar, 100 µm.

the saline and heroin pairings on the first day of conditioning (Session 1), and the saline and heroin pairings on the fourth day of conditioning (Session 4; Fig. 3*A*,*B*). For these recordings, pairs of rats were injected with saline (09:00) or heroin (13:00), connected to the photometry system via a branching fiber optic patch cord, and immediately placed into CPP chambers. As recordings were not started until ~1 min after rats received intraperitoneal injections, normalization of photometry signals was done relative to the entirety of the conditioning session, rather than using a pre-injection baseline period as a reference. A two-way repeated-measures ANOVA revealed a significant session × drug interaction on the frequency of DA events ($F_{(1,8)} = 11.94$, $p = 0.0086$), with more DA events after heroin in Session 4 compared with both heroin in Session 1 ($q = 0.0058$, $p = 0.0010$) and saline in Session 4 ($q = 0.026$, $p = 0.013$; Fig. 3*C*). Kolmogorov–Smirnov tests on the cumulative distribution of event amplitudes in each session revealed significant heroin-induced leftward shifts in both Session 1 ($D = 0.20$, $p < 0.0001$) and Session 4 ($D = 0.24$, $p < 0.0001$), indicative of heroin-induced suppression of large-amplitude DA events (Fig. 3*D*,*E*). Indeed, two-way repeated-measures ANOVAs revealed significant main effects of drug on both the mean amplitude of DA events ($F_{(1,8)} = 13.10$, $p = 0.0068$) and the variance of DA event amplitudes ($F_{(1,8)} = 25.02$, $p = 0.0010$), with reduced amplitude (Session 1, $q = 0.0028$, $p = 0.0014$; Session 4, $q = 0.0010$, $p = 0.0003$) and variance (Session 1, $q = 0.0094$, $p = 0.0031$; Session 4, $q = 0.034$, $p = 0.022$) of DA events after heroin (Fig. 3*F*,*G*).

### NAc DA signaling is greater when entering a heroin-paired than a saline-paired context

Photometry signals were also recorded during both the initial ("pretest") and final ("post-test") preference tests to assess the role of NAc DA signaling in the expression of a heroin CPP (Fig. 4*A*,*B*). Transitions between the center chamber and the saline- and heroin-paired chambers were time-stamped and aligned to photometry signals, and the 6 s window centered around each transition was isolated for analysis (Fig. 4*C*,*D*). A paired *t* test revealed a significant increase in preference for the heroin-paired

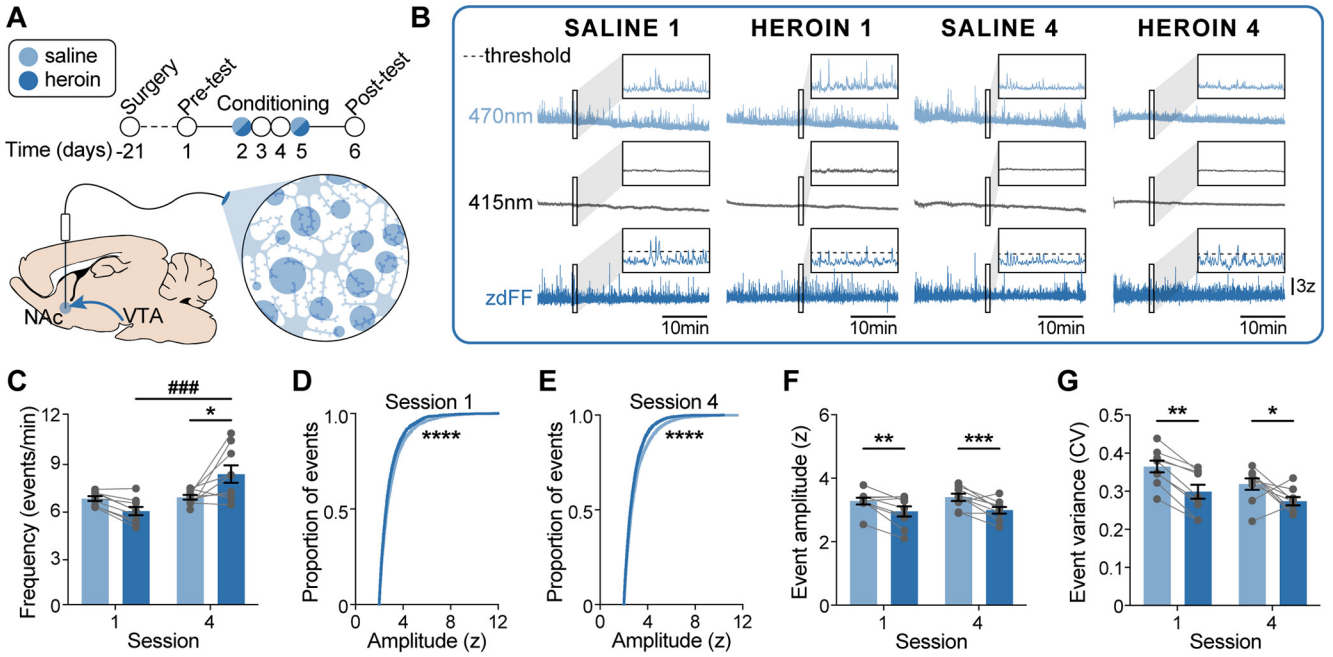


**Figure 3.** Heroin conditioning sensitizes NAc DA signaling. ***A***, Timeline for NAc DA recordings during CPP conditioning sessions. ***B***, Representative DA signals collected during the first and fourth saline and heroin sessions. Inset, 60 s. Top, Raw experimental signal. Middle, Raw reference signal. Bottom, Normalized dLight1.3b signal. ***C***, Heroin significantly enhanced the frequency of DA events in Session 4. ***D***, ***E***, Heroin significantly reduced the frequency of large-amplitude DA events in Sessions 1 and 4. ***F***, Heroin significantly reduced the mean amplitude of DA events. ***G***, Heroin had no effect on the variance of DA event amplitudes. $n = 9$ rats. $^{*}p < 0.05$; $^{**}p < 0.01$; $^{***}p < 0.001$; $^{****}p < 0.0001$ (saline vs heroin). $^{\#\#\#}p < 0.001$ (Session 1 vs Session 4).

chamber during the post-test compared with the pretest ($t_{(8)}$ = 5.35, $p = 0.0007$; Fig. 4*E*), and an unpaired *t* test found no sex difference in final preference for the heroin-paired chamber ($t_{(7)}$ = 0.51, $p = 0.62$; data not shown). A two-way repeated-measures ANOVA revealed a significant chamber × test interaction for DA signaling at the moment of chamber entry ($F_{(1,6)}$ = 71.34, $p < 0.0001$), with weaker DA signaling during entry to the saline-paired chamber (pre vs post, $q = 0.022$, $p = 0.015$) and greater DA signaling during entry to the heroin-paired chamber (pre vs post, $q = 0.0004$, $p = 0.0001$; saline vs heroin, $q = 0.0002$, $p < 0.0001$) during the post-test (Fig. 4*F*). Similarly, a two-way repeated-measures ANOVA revealed a significant chamber × test interaction for DA signaling across the entire entry window ($F_{(1,6)}$ = 64.60, $p = 0.0002$), with weaker DA signaling during entry to the saline-paired chamber (pre vs post, $q = 0.024$, $p = 0.016$) and greater DA signaling during entry to the heroin-paired chamber (pre vs post, $q = 0.0006$, $p = 0.0002$; saline vs heroin, $q = 0.0002$, $p < 0.0001$) during the post-test (Fig. 4*G*). Finally, two-way repeated-measures ANOVAs revealed a significant chamber × test interaction for DA signaling at the moment of chamber exit ($F_{(1,6)}$ = 8.91, $p = 0.025$) but not across the entire exit window ($F_{(1,6)}$ = 0.027, $p = 0.87$), with significantly weaker DA signaling during exit from the heroin-paired chamber during the post-test (pre vs post, $q = 0.046$, $p = 0.0086$; saline vs heroin, $q = 0.046$, $p = 0.015$; Fig. 4*H*,*I*).

### Heroin conditioning increases the frequency of NAc dMSN signaling

Next, photometry signals were recorded throughout conditioning to assess the role of NAc dMSN signaling in the development of a heroin CPP (Fig. 5*A*,*B*). A two-way repeated-measures ANOVA on the frequency of dMSN $Ca^{2+}$ events revealed a significant session × drug interaction ($F_{(1,11)}$ = 17.44, $p = 0.0015$), with a decrease in dMSN signaling events during the first heroin session (saline 1 vs heroin 1, $q = 0.024$, $p = 0.0040$) but an increase in dMSN signaling events during the fourth heroin session (saline four vs heroin 4, $p = 0.029$, $p = 0.012$), as well a decrease in dMSN signaling events during the fourth saline session (saline 1 vs saline 4, $q = 0.029$, $p = 0.014$; Fig. 5*C*). Kolmogorov–Smirnov tests on the cumulative distribution of dMSN event amplitudes revealed significant heroin-induced leftward shifts in both Session 1 ($D = 0.63$, $p < 0.0001$) and Session 4 ($D = 0.49$, $p < 0.0001$), indicative of heroin-induced suppression of large-amplitude dMSN signaling events (Fig. 5*D*,*E*). Accordingly, a two-way repeated-measures ANOVA revealed a significant main effect of drug on the mean amplitude of dMSN events ($F_{(1,11)}$ = 17.15, $p = 0.0015$) but not the variance of dMSN event amplitudes ($F_{(1,11)}$ = 0.018, $p = 0.89$), with significant heroin-induced reductions in amplitude in both Session 1 (saline 1 vs heroin 1, $q = 0.013$, $p = 0.0062$) and Session 4 (saline 4 vs heroin 4, $q = 0.013$, $p = 0.0063$; Fig. 5*F*,*G*).

### NAc dMSN signaling is greater when entering a heroin-paired than a saline-paired context

Photometry signals were also recorded during the preference tests to assess the role of NAc dMSN signaling in the expression of a heroin CPP (Fig. 6*A*–*D*). A paired *t* test revealed a significant increase in preference for the heroin-paired chamber during the post-test compared with the pretest ($t_{(11)}$ = 3.17, $p = 0.009$; Fig. 6*E*), and an unpaired *t* test found no sex difference in final preference for the heroin-paired chamber ($t_{(10)}$ = 0.16, $p = 0.88$; data not shown). A two-way repeated-measures ANOVA revealed a significant chamber × test interaction for dMSN signaling at the moment of chamber entry ($F_{(1,11)}$ = 126.5, $p < 0.0001$), with weaker dMSN signaling during entry to the saline-paired chamber (pre vs post, $q = 0.0007$, $p = 0.0005$) and greater dMSN signaling during entry to the heroin-paired chamber (pre vs post and saline vs heroin, $q < 0.0001$, $p < 0.0001$) during the post-test (Fig. 6*F*). Similarly, a two-way repeated-measures ANOVA revealed a significant chamber × test interaction for dMSN

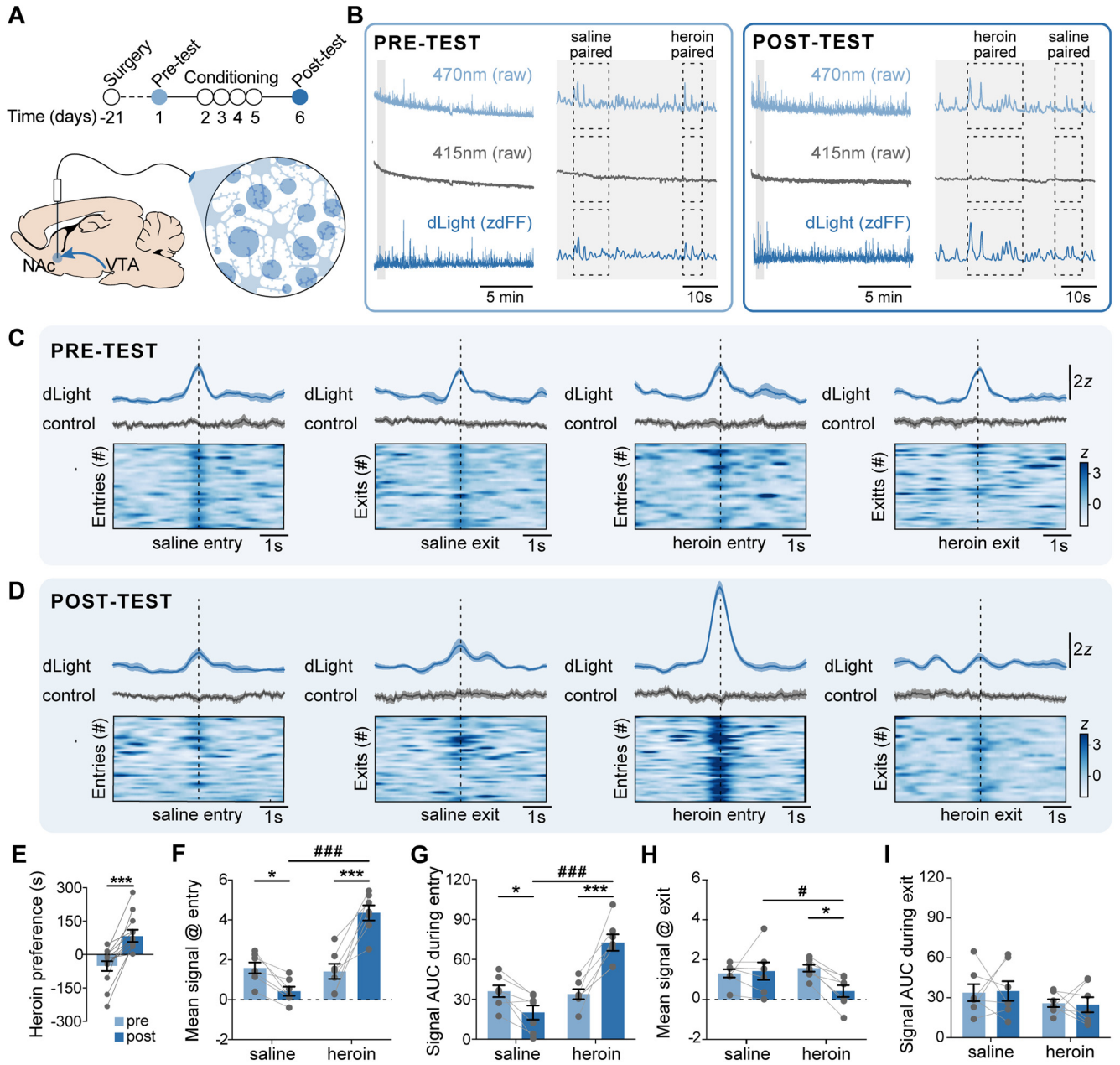


**Figure 4.** NAc DA signaling is stronger when entering a heroin-paired than a saline-paired context. ***A***, Timeline for NAc DA recordings during CPP test sessions. ***B***, Representative DA signals collected during the pretest and post-test. Inset, 45 s. Top, Raw experimental signal. Middle, Raw reference signal. Bottom, Normalized dLight1.3b signal. ***C***, ***D***, DA signals aligned to transitions between the center and outer chambers during the pretest and post-test. Top. Mean *z*-scored dLight1.3b and control signals across all transitions of each type. Bottom, Heatmap of individual transitions ($n = 45$ transitions each). ***E***, Heroin conditioning significantly increased preference for the heroin-paired chamber. ***F***, ***G***, DA signals during the post-test were significantly greater when entering the heroin-paired chamber than the saline-paired chamber. ***H***, ***I***, DA signals during the post-test were significantly weaker when exiting the heroin-paired chamber than the saline-paired chamber. AUC, Area under the curve; control: *z*-scored reference signal. $n = 9$ rats. $^{*}p < 0.05$; $^{***}p < 0.001$; $^{\#}p < 0.05$; $^{\#\#\#}p < 0.001$ (saline-paired vs heroin-paired).

signaling across the entire entry window ($F_{(1,11)} = 18.25$, $p = 0.0013$), with greater dMSN signaling during entry to the heroin-paired chamber during the post-test (pre vs post, $q = 0.0059$, $p = 0.0020$; saline vs heroin, $q = 0.0042$, $p = 0.0007$; Fig. 6*G*). Further, a two-way repeated-measures ANOVA revealed a significant chamber × test interaction for dMSN signaling at the moment of chamber exit ($F_{(1,11)} = 37.76$, $p < 0.0001$), with weaker dMSN signaling during exit from the heroin-paired chamber during the post-test (pre vs post and saline vs heroin, $q < 0.0001$, $p < 0.0001$; Fig. 6*H*). Finally, a two-way repeated-measures ANOVA revealed a significant chamber × test interaction for dMSN signaling across the entire exit window ($F_{(1,11)} = 8.11$, $p = 0.016$), with significantly weaker dMSN signaling during exit from the heroin-paired chamber during the post-test (pre vs post, $q = 0.0048$, $p = 0.0024$; saline vs heroin, $q = 0.0048$, $p = 0.0013$; Fig. 6*I*).

### Heroin conditioning decreases the frequency of NAc iMSN signaling

Finally, photometry signals were recorded throughout conditioning to assess the role of NAc iMSN signaling in the development of a heroin CPP (Fig. 7*A*,*B*). A two-way repeated-measures ANOVA on the frequency of iMSN $Ca^{2+}$ events revealed a significant session × drug interaction ($F_{(1,9)} = 18.73$, $p = 0.0019$),

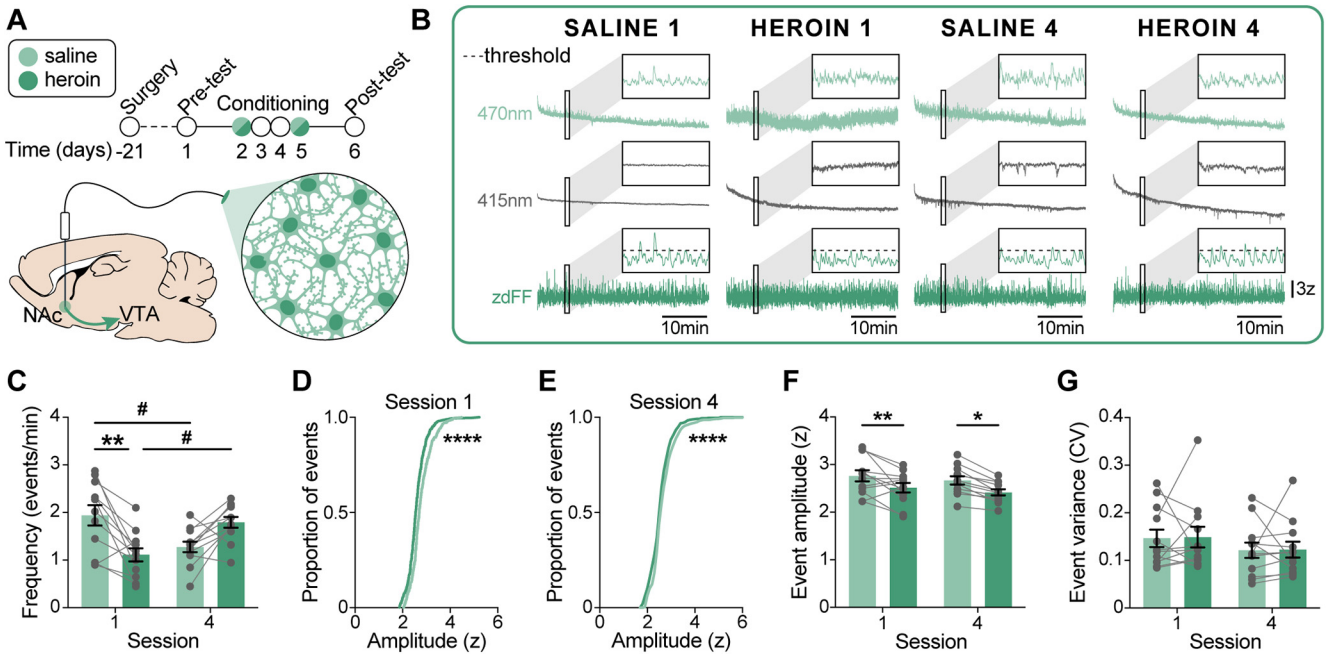


**Figure 5.** Heroin conditioning enhances NAc dMSN signaling. ***A***, Timeline for NAc dMSN recordings during CPP conditioning sessions. ***B***, Representative dMSN signals collected during the first and fourth saline and heroin sessions. Inset, 60 s. Top, Raw experimental signal. Middle, Raw reference signal. Bottom, Normalized GCaMP6s signal. ***C***, Frequency of dMSN events was significantly reduced by heroin in Session 1 but significantly enhanced by heroin in Session 4. ***D***, ***E***, Heroin significantly reduced the proportion of large-amplitude dMSN events in Sessions 1 and 4. ***F***, Heroin significantly reduced the mean amplitude of dMSN events in Sessions 1 and 4. ***G***, Heroin had no effect on the variance of dMSN event amplitudes. $n = 12$ rats. $^{*}p < 0.05$; $^{**}p < 0.01$; $^{****}p < 0.0001$ (saline vs heroin); $^{\#}p < 0.05$ (Session 1 vs Session 4).

with an increase in iMSN signaling events during the first heroin session (saline 1 vs heroin 1, $q = 0.027$, $p = 0.0089$) but a decrease in iMSN signaling events during the fourth heroin session (saline four vs heroin 4, $q = 0.042$, $p = 0.021$; heroin 1 vs heroin 4, $q = 0.0095$, $p = 0.0016$; Fig. 7*C*). Moreover, Kolmogorov–Smirnov tests on the cumulative distribution of iMSN event amplitudes revealed a heroin-induced rightward shift in Session 1 ($D = 0.48$, $p < 0.0001$) but a leftward shift in Session 4 ($D = 0.45$, $p < 0.0001$; Fig. 7*D*,*E*). A two-way repeated-measures ANOVA on the mean amplitude of iMSN events revealed both a significant main effect of session ($F_{(1,9)} = 10.59$, $p = 0.0099$) and a significant session × drug interaction ($F_{(1,9)} = 15.11$, $p = 0.0037$), with greater iMSN amplitudes after heroin in Session 1 (saline 1 vs heroin 1, $q = 0.0091$, $p = 0.0045$) but weaker iMSN amplitudes after heroin in Session 4 (heroin 1 vs heroin 4, $q = 0.0006$, $p = 0.0001$; Fig. 7*F*). However, two-way repeated-measures ANOVAs on the variance of iMSN event amplitudes found no significant main effect of drug ($F_{(1,9)} = 2.73$, $p = 0.13$) and no significant session × drug interaction ($F_{(1,9)} = 0.86$, $p = 0.38$; Fig. 7*G*).

### NAc iMSN signaling is greater when exiting a heroin-paired than a saline-paired context

Photometry signals were also recorded during the preference tests to assess the role of NAc iMSN signaling in the expression of a heroin CPP (Fig. 8*A*–*D*). A paired *t* test revealed a significant increase in preference for the heroin-paired chamber during the post-test compared with the pretest ($t_{(10)} = 3.28$, $p = 0.0084$; Fig. 8*E*), and an unpaired *t* test found no sex difference in final preference for the heroin-paired chamber ($t_{(8)} = 0.42$, $p = 0.68$; data not shown). A two-way repeated-measures ANOVA revealed a significant test × chamber interaction for iMSN signaling at the moment of chamber entry ($F_{(1,9)} = 13.22$, $p = 0.0054$), with weaker iMSN signaling during entry to the heroin-paired chamber in the post-test (pre vs post, $q = 0.044$, $p = 0.015$; saline vs heroin, $q = 0.0051$, $p = 0.0008$; Fig. 8*F*). Similarly, a two-way repeated-measures ANOVA revealed a significant test × chamber interaction for iMSN signaling across the entire entry window ($F_{(1,9)} = 13.09$, $p = 0.0056$), with weaker iMSN signaling during entry to the heroin-paired chamber in the post-test (pre vs post, $q = 0.0046$, $p = 0.0008$; saline vs heroin, $q = 0.041$, $p = 0.016$; Fig. 8*G*). Further, a two-way repeated-measures ANOVA revealed a significant test × chamber interaction for iMSN signaling at the moment of chamber exit ($F_{(1,9)} = 9.28$, $p = 0.014$), with greater iMSN signaling during exit from the heroin-paired chamber in the post-test (pre vs post, $q = 0.030$, $p = 0.0099$; saline vs heroin, $q = 0.019$, $p = 0.0032$; Fig. 8*H*). Finally, a two-way repeated-measures ANOVA revealed a significant test × chamber interaction for iMSN signaling across the entire exit window ($F_{(1,9)} = 14.22$, $p = 0.0044$), with greater iMSN signaling during exit from the heroin-paired chamber in the post-test (pre vs post, $q = 0.030$, $p = 0.0099$; saline vs heroin, $q = 0.022$, $p = 0.0036$; Fig. 8*I*).

### Buprenorphine pretreatment blocks the development of heroin CPP

Buprenorphine is used for opioid replacement therapy because of its ability to weakly activate $\mu$ opioid receptor signaling and prevent the binding of other opioids (e.g., heroin), and was recently shown to occlude heroin-evoked DA release into the NAc (Isaacs et al., 2020). To determine whether buprenorphine could similarly prevent the acquisition of heroin CPP, rats underwent a modified CPP procedure with 0 or 0.2 mg/kg buprenorphine given 10 min before each conditioning session (Fig. 9*A*). A two-way repeated-measures ANOVA revealed a significant dose × test interaction on heroin preference ($F_{(1,14)} =$

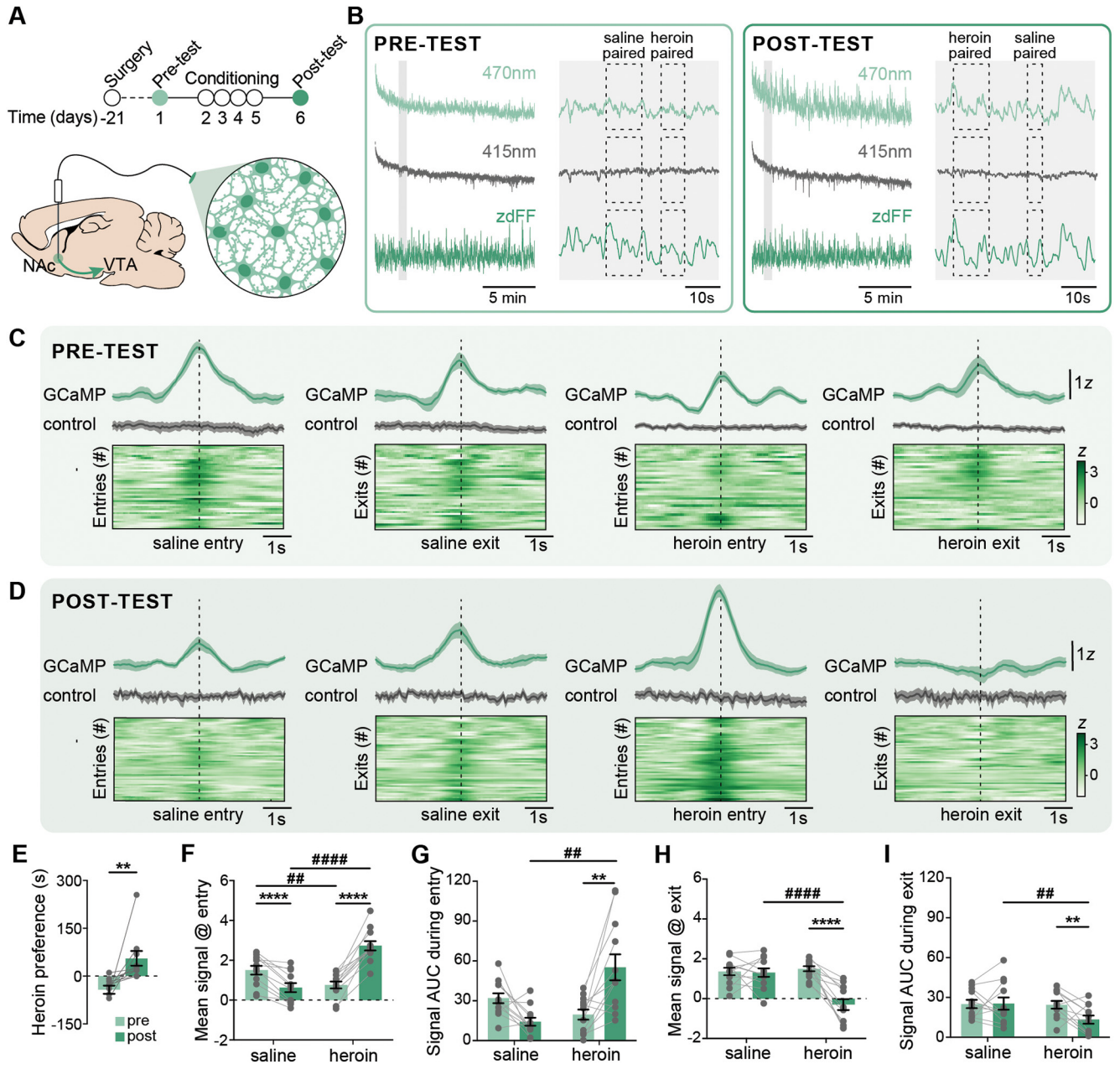


**Figure 6.** NAc dMSN signaling is stronger when entering a heroin-paired than a saline-paired context. ***A***, Timeline for NAc dMSN recordings during CPP test sessions. ***B***, Representative dMSN signals collected during the pretest and post-test. Inset, 45 s. Top, Raw experimental signal. Middle, Raw reference signal. Bottom, Normalized GCaMP6s signal. ***C***, ***D***, dMSN signals aligned to transitions between the center and outer chambers during the pretest and post-test. Top, Mean *z*-scored GCaMP6s and control signals across all transitions of each type. Bottom, Heatmap of individual transitions ($n = 60$ transitions each). ***E***, Heroin conditioning significantly increased preference for the heroin-paired chamber. ***F***, ***G***, dMSN signals during the post-test were significantly greater when entering the heroin-paired than the saline-paired chamber. ***H***, ***I***, dMSN signals during the post-test were significantly weaker when exiting the heroin-paired than the saline-paired chamber. AUC, Area under the curve; control, *z*-scored reference signal. $n = 12$ rats. $^{**}p < 0.01$; $^{****}p < 0.0001$; $^{\#\#}p < 0.01$; $^{\#\#\#\#}p < 0.0001$ (saline-paired vs heroin-paired).

8.52, $p = 0.012$), with an increase in time spent in the heroin-paired chamber for rats pretreated with 0 mg/kg buprenorphine ($p = 0.0086$) but not 0.2 mg/kg buprenorphine ($p = 0.73$; Fig. 9*B*). Moreover, an unpaired *t* test revealed significantly lower final preference for the heroin-paired chamber in rats pretreated with 0.2 mg/kg buprenorphine ($t_{(14)} = 2.83$, $p = 0.014$; Fig. 9*C*). To assess the impact of buprenorphine pretreatment during conditioning on NAc activation during the final preference test, rats were killed 30 min after the final preference test, and brains were processed for Fos immunohistochemistry. Unpaired *t* tests revealed significantly lower levels of Fos activation in both the NAc core ($t_{(14)} = 4.78$, $p = 0.0003$) and NAc shell ($t_{(14)} = 6.20$, $p < 0.0001$) for rats pretreated with 0.2 mg/kg buprenorphine during conditioning (Fig. 9*D–G*). Importantly, two-way ANOVAs revealed no main effect of sex on final preference for the heroin-paired chamber ($F_{(1,12)} = 1.40$, $p = 0.26$) or Fos activation in the NAc core ($F_{(1,12)} = 1.09$, $p = 0.32$) or NAc shell ($F_{(1,12)} = 0.26$, $p = 0.62$).

## Discussion

Here, we sought to examine the role of NAc signaling in the acquisition and expression of heroin CPP by coupling fiber

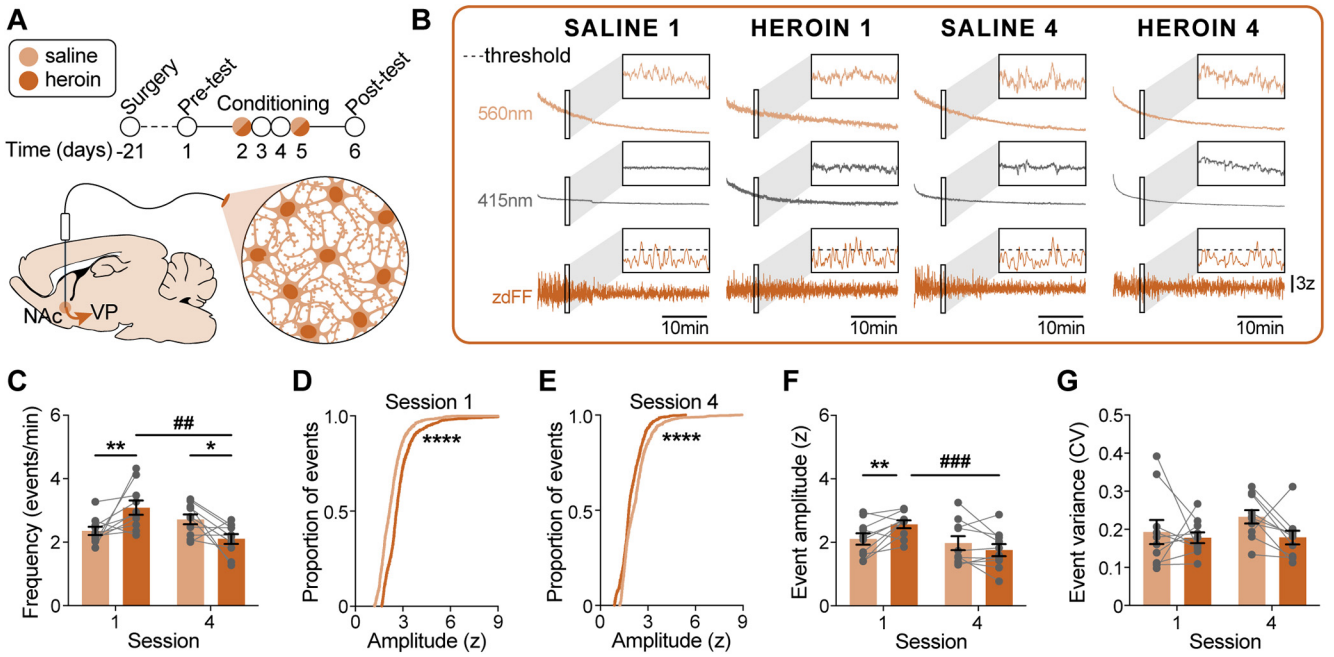


**Figure 7.** Heroin conditioning suppresses NAc iMSN signaling. ***A***, Timeline for NAc iMSN recordings during CPP conditioning sessions. ***B***, Representative iMSN signals collected during the first and fourth saline and heroin sessions. Inset, 60 s. Top, Raw experimental $p < 0.01$. Middle, Reference signal. Bottom, Normalized RCaMP1b signal. ***C***, Frequency of iMSN events was significantly enhanced by heroin in Session 1 but significantly reduced by heroin in Session 4. ***D***, ***E***, Heroin significantly increased the proportion of large-amplitude iMSN events in Session 1, but significantly decreased the proportion of large-amplitude iMSN events in Session 4. ***F***, Heroin significantly increased the mean amplitude of iMSN events in Session 1, but significantly reduced the mean amplitude of iMSN events in Session 4. ***G***, Heroin had no effect on the variance of iMSN event amplitudes. $n = 10$ rats. $^{*}p < 0.05$; $^{**}p < 0.01$; $^{****}p < 0.0001$ (saline vs heroin); $^{\#\#}p < 0.01$; $^{\#\#\#}p < 0.001$ (Session 1 vs Session 4).

photometry recordings with a heroin CPP procedure that induces Fos activation in the NAc during expression of heroin CPP. We identified differences in the neural response to heroin over the course of conditioning, with suppression of NAc activity during early conditioning but enhancement of NAc activity during late conditioning. Next, we demonstrated greater DA and dMSN $Ca^{2+}$ signaling and weaker iMSN $Ca^{2+}$ signaling when entering a heroin-paired context compared with a saline-paired context, as well as greater iMSN signaling and weaker DA and dMSN signaling when exiting a heroin-paired context compared with a saline-paired context. Finally, we show that buprenorphine pretreatment during conditioning is sufficient to prevent the expression of heroin CPP and block Fos activation in the NAc. Together, these data reveal a central role for the NAc in the reinforcing effects of heroin, in accordance with the hypothesis that an imbalance in signaling between the NAc direct and indirect pathways drives addictive behaviors.

### Dopaminergic modulation in the NAc contributes to heroin conditioning

While the contribution of DA to the rewarding effects of most potentially addictive drugs (e.g., psychostimulants, nicotine) is well established (Crummy et al., 2020), the role of DA in opioid reward is more complicated (Badiani et al., 2011). Opioids increase phasic DA release, and both D1 receptor blockade and D2 receptor deletion blocks morphine reward (Johnson and North, 1992; Shippenberg et al., 1993; Maldonado et al., 1997; Sellings and Clarke, 2003). However, bilateral 6-OHDA lesions of the NAc can block or have no effect on morphine reward (Shippenberg et al., 1993; Sellings and Clarke, 2003), and chronic blockade of both D1 and D2 receptors potentiates the rewarding effects of low doses of heroin (Stinus et al., 1989). During conditioning, we identified noteworthy effects of heroin on DA signaling, including a reduction in large-amplitude DA events during both early and late conditioning sessions, a reduction in the frequency of DA events during early conditioning, and an enhancement in the frequency of DA events during late conditioning. This shift from suppression to elevation across conditioning sessions suggests sensitization of the dopaminergic response to heroin and supports a role for DA in the acquisition of heroin CPP. During the CPP test, we detected a significant increase in DA signaling preceding entries to the heroin-paired chamber, as well as significant decreases in DA signaling preceding exits from the heroin-paired chamber and entries to the saline-paired chamber, indicating emergent selectivity for DA signaling in response to a heroin-paired context.

### An imbalance in NAc activity develops during heroin conditioning

The ability of DA to alter overall NAc activity is dependent not only on dopaminergic modulation of individual MSNs but also on the network implications of such modulation. Although dMSNs and iMSNs can be differentiated according to their downstream targets (VTA and VP, respectively), both subtypes of MSNs are heavily interconnected in a local microcircuit of lateral inhibition within the NAc (Burke et al., 2017). Indeed, although dMSNs are more likely to collateralize with other dMSNs than iMSNs (Taverna et al., 2008), D2 receptor-mediated disinhibition of iMSN lateral inhibition onto dMSNs is necessary for the locomotor sensitizing effects of cocaine (Dobbs et al., 2016). An imbalance between dMSNs and iMSNs can thereby shape the ability of DA to modulate NAc activity, with the overall balance in signaling guiding vulnerability to the reinforcing effects of drugs.

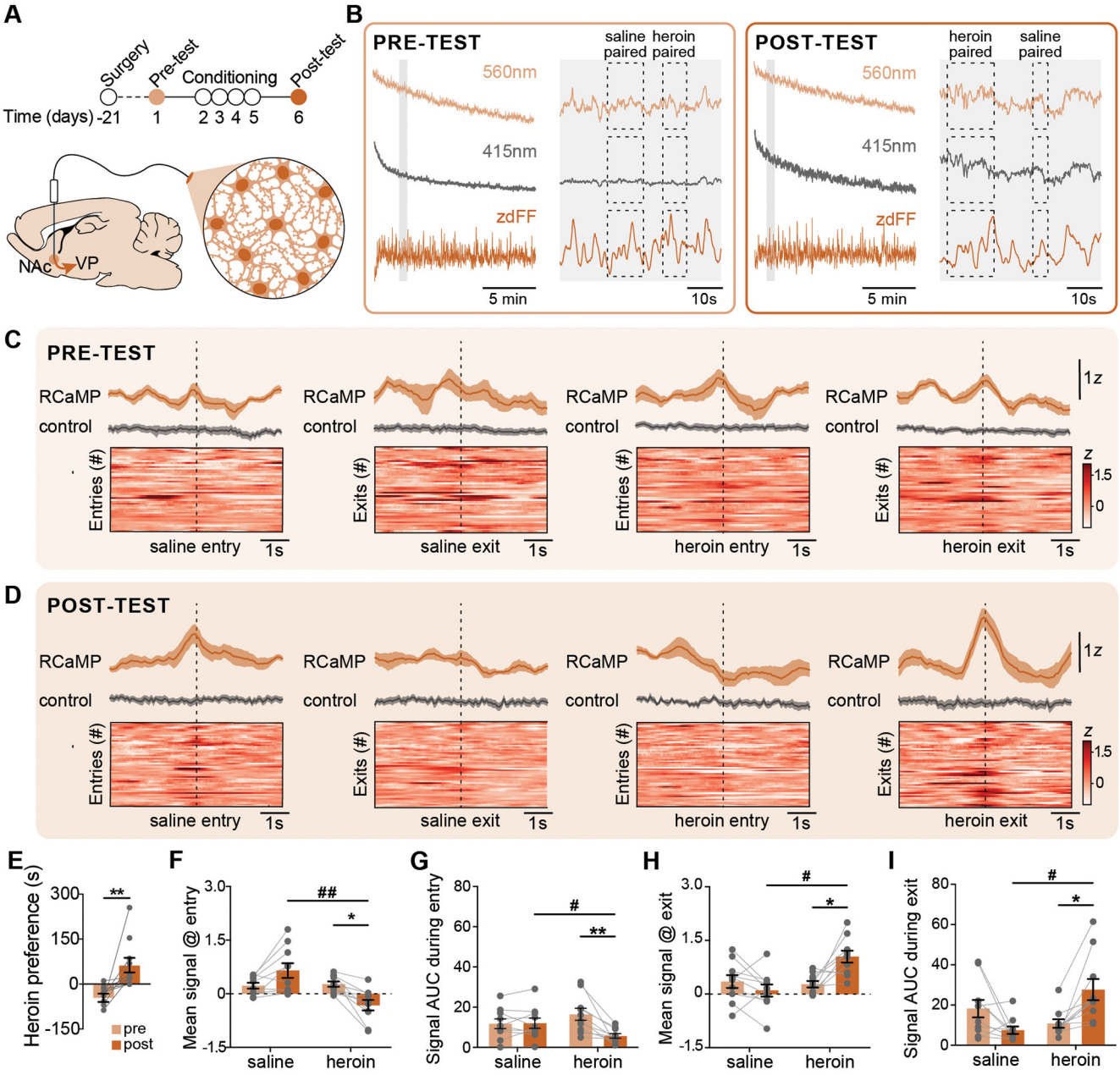


**Figure 8.** NAc iMSN signaling is weaker when entering a heroin-paired than a saline-paired context. ***A***, Timeline for NAc iMSN recordings during CPP test sessions. ***B***, Representative iMSN signals collected during the pretest and post-test. Inset, 45 s. Top, Raw experimental signal. Middle, Raw reference signal. Bottom, Normalized RCaMP1b signal. ***C***, ***D***, iMSN signals aligned to transitions between the center and outer chambers during the pre-test and post-test. Top, Mean *z*-scored RCaMP1b and control signals across all transitions of each type. Bottom, Heatmap of individual transitions ($n = 50$ transitions each). ***E***, Heroin conditioning significantly increased preference for the heroin-paired chamber. ***F***, ***G***, iMSN signals during the post-test were significantly weaker when entering the heroin-paired than the saline-paired chamber. ***H***, ***I***, iMSN signals during the post-test were significantly greater when exiting the heroin-paired than the saline-paired chamber. AUC, Area under the curve; control, *z*-scored reference signal. $n = 10$ rats. $^{*}p < 0.05$; $^{**}p < 0.01$ (pretest vs post-test); $^{\#}p < 0.05$; $^{\#\#}p < 0.01$ (saline-paired vs heroin-paired).

We observed a shift in the response of NAc iMSNs to heroin over the course of conditioning, with a prominence of iMSN signaling during early conditioning (i.e., enhanced iMSN frequency and amplitudes) and a suppression of iMSN signaling during late conditioning (i.e., reduced iMSN frequency and amplitudes). This inhibition of iMSN signaling, mediated in part by an enhanced dopaminergic response to heroin during late conditioning, would release nearby dMSNs from tonic lateral inhibition, allowing direct pathway signaling to dominate. Interestingly, however, we did not observe a sensitized dMSN response to heroin over the course of conditioning; rather, we observed a transient reduction in dMSN signaling during the fourth saline session, indicating a weakening of basal dMSN tone over the course of heroin conditioning. In addition to heroin-induced disruptions in NAc activity over the course of conditioning, we identified context-dependent changes in MSN signals after conditioning. Specifically, dMSN signals were stronger when entering the heroin-paired context, but weaker when exiting the heroin-paired or entering the saline-paired contexts. Conversely, iMSN signals were weakened when entering the heroin-paired context, but stronger when exiting the heroin-paired or entering the saline-paired contexts. These data indicate selective tuning of dMSNs to the heroin-paired context, and are consistent with previous findings of elevated dMSN signaling during re-exposure to a cocaine-paired context (Calipari et al., 2016).

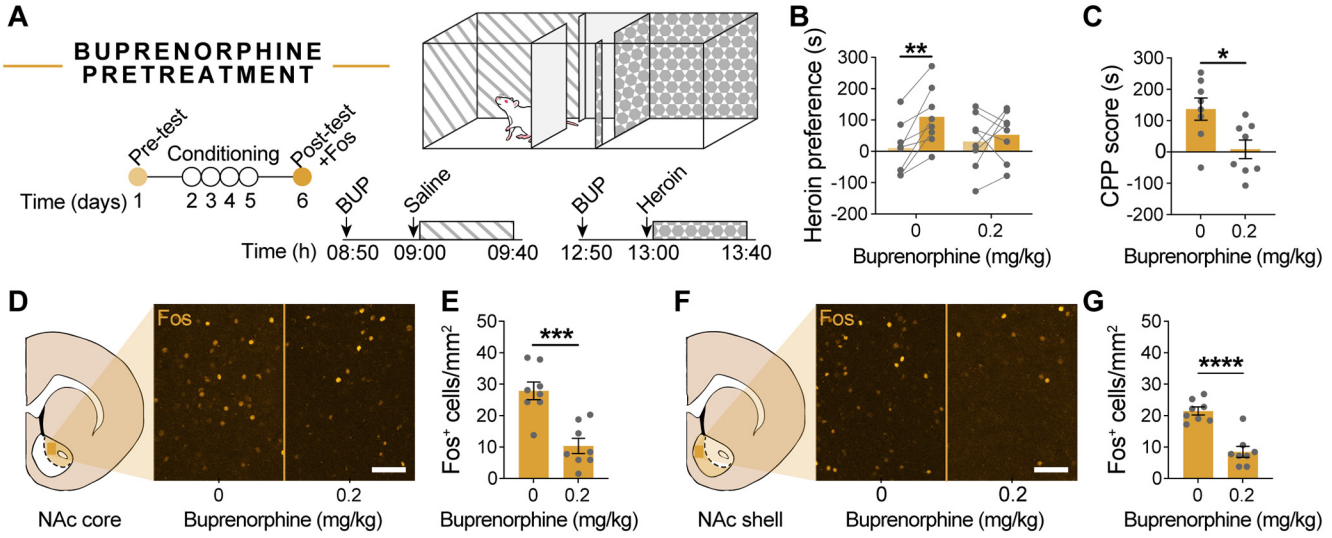


**Figure 9.** Acquisition of heroin CPP is blocked by buprenorphine. ***A***, Timeline for buprenorphine experiment. Testing was performed as described in Figure 1, but rats received buprenorphine pretreatment 10 min before each conditioning session. ***B***, ***C***, Rats pretreated with 0.2 mg/kg buprenorphine spent significantly less time in the heroin-paired chamber during the post-test than those pretreated with 0 mg/kg buprenorphine and did not develop a preference for the heroin-paired chamber. ***D–G***, Representative images and quantification of Fos in the NAc. Rats pretreated with 0.2 mg/kg buprenorphine had significantly less Fos in both subregions of the NAc than those pretreated with 0 mg/kg buprenorphine. $n = 8$/group. Scale bar, 50 μm. $^{*}p < 0.05$. $^{**}p < 0.01$. $^{***}p < 0.001$. $^{****}p < 0.0001$.

### Disrupting opioid signaling prevents development of heroin CPP

In our final experiment, we show that pretreatment with buprenorphine during conditioning blocked the development of a heroin CPP and associated Fos activity in the NAc. Although buprenorphine weakly activates $\mu$ opioid receptors to mildly elevate DA release, it also prevents heroin from binding to the same receptors and driving larger phasic DA release (Isaacs et al., 2020). The buprenorphine dose used in the present study was selected based on a previous report that described a bell-shaped curve for buprenorphine-stimulated DA release into the NAc, with significant increases in DA release with 0.01-0.04 mg/kg buprenorphine, but no change in DA release with 0.18-0.7 mg/kg buprenorphine (Isaacs et al., 2020). Moreover, twice daily injections of 0.1-0.4 mg/kg buprenorphine are sufficient to attenuate cocaine self-administration in rats, with no differences observed between 0.1 and 0.4 mg/kg (Carroll and Lac, 1992). Thus, our dose of buprenorphine administered before each conditioning session likely produced comparably low levels of DA release in both chambers, preventing the acquisition of a strong conditioned response to heroin.

### Technical considerations

Although dMSNs and iMSNs have canonically been assumed to project exclusively to the VTA and VP, respectively, growing evidence has demonstrated that dMSNs project equally strong to the VTA and the VP in mice (Kupchik et al., 2015; Creed et al., 2016). Importantly, the viral strategy used here has been shown to target largely nonoverlapping populations of neurons in the NAc of rats, with bidirectional control over cue-induced heroin-seeking (O'Neal et al., 2020). In the present study, we not only did not observe coexpression of GCaMP6s and RCaMP1b within the NAc, but we also observed oppositional dMSN and iMSN $Ca^{2+}$ signals during transitions in the post-test, similar to what has previously been reported during cocaine CPP (Calipari et al., 2016). Furthermore, although dual-color imaging runs the risk of signal crosstalk and contamination (Meng et al., 2018), our dMSN-GCaMP6s and iMSN-RCaMP1b signals were highly uncorrelated throughout testing (Fig. 2*J*). There is also concern that the viral strategy used to target dMSNs may have led to undesired expression of GCaMP6s in DA terminals in the NAc. While retrograde AAVs have a higher tropism for axon terminals, some evidence suggests they may also infect cell bodies at the site of infusion (Tervo et al., 2016). Moreover, AAV8s have been shown to undergo some degree of retrograde transport, particularly when infused near DA terminals (Masamizu et al., 2011; Löw et al., 2013). However, using TH immunohistochemistry, we did not detect GCaMP6s expression in either DA terminals in the NAc or in DA cell bodies in the VTA (data not shown). It is also important to note that, for all photometry experiments, the 415 nm signal was used primarily to correct for photobleaching, autofluorescence, and motion artifacts in experimental signals, rather than as a true isosbestic signal to account for calcium-independent fluorescence. While this approach has been used successfully in previous photometry studies (e.g., Lerner et al., 2015; Corre et al., 2018; Patriarchi et al., 2020), it is possible that the reference channel may have contained some degree of biological signal that was subtracted during normalization. However, the precise isosbestic point for many biosensors, including dLight1.3b and RCaMP1b, has not been fully characterized, and the isosbestic point for a given biosensor can shift depending on intracellular pH (Barnett et al., 2017; Siciliano and Tye, 2019). Thus, raw 415 nm signals have been included alongside raw experimental signals and normalized signals throughout all photometry figures to allow visual comparison of raw and normalized signals. Additionally, a recent study using DA imaging in the NAc medial shell following heroin administration reported a significant rise in tonic DA signaling over a period of minutes, relative to a pre-injection baseline (Corre et al., 2018). While we did not observe a similar effect on DA signaling during conditioning, we believe this is largely because of lack of a pre-injection baseline in the study design. Future work should expand on these data to better understand how heroin conditioning is altering tonic signaling in the NAc, in addition to phasic changes. It should also be noted that signal normalization preceded event quantification and analyses for all photometry

data discussed herein, so differences in activity between sessions may have influenced analyses. This is particularly relevant for conditioning sessions, where a large shift in signal-to-noise between sessions could affect detection and quantification of events. Although the dynamic range of our photometry signals was comparable across sessions for all subjects, this is an important caveat to keep in mind when interpreting these findings.

In conclusion, together, these data highlight a central role for NAc dMSN, iMSN, and DA signaling in the acquisition and expression of heroin CPP. Future work will investigate the role of NAc signaling in encoding individual vulnerability to the rewarding and motivating effects of heroin, with a particular focus on the relative strength of dMSNs and iMSNs between individuals sensitive to versus resistant to the conditioned reinforcement produced by heroin.

## References


Badiani A, Belin D, Epstein D, Calu D, Shaham Y (2011) Opiate versus psychostimulant addiction: the differences do matter. Nat Rev Neurosci 12:685–670.

Bailey CH, Giustetto M, Huang YY, Hawkins RD, Kandel ER (2000) Is heterosynaptic modulation essential for stabilizing Hebbian plasticity and memory. Nat Rev Neurosci 1:11–20.

Bardo MT, Rowlett JK, Harris MJ (1995) Conditioned place preference using opiate and stimulant drugs: a meta-analysis. Neurosci Biobehav Rev 19:39–51.

Barnett LM, Hughes TE, Drobizhev M (2017) Deciphering the molecular mechanism responsible for GCaMP6m's $Ca^{2+}$-dependent change in fluorescence. PLoS One 12:e0170934.

Bock R, Hoon Shin J, Kaplan AR, Dobi A, Markey E, Kramer PF, Gremel CM, Christensen CH, Adrover MF, Alvarez VA (2013) Strengthening the accumbal indirect pathway promotes resilience to compulsive cocaine use. Nat Neurosci 16:632–638.

Burke DA, Rotstein HG, Alvarez VA (2017) Striatal local circuitry: a new framework for lateral inhibition. Neuron 96:267–284.

Calabresi P, Picconi B, Tozzi A, Ghiglieri V, Di Filippo M (2014) Direct and indirect pathways of basal ganglia: a critical reappraisal. Nat Neurosci 17:1022–1030.

Calipari ES, Bagot RC, Purushothaman I, Davidson TJ, Yorgason JT, Peña CJ, Walker DM, Pirpinias ST, Guise KG, Ramakrishnan C, Deisseroth K, Nestler EJ (2016) In vivo imaging identifies temporal signature of D1 and D2 medium spiny neurons in cocaine reward. Proc Natl Acad Sci USA 113:2726–2731.

Carroll ME, Lac ST (1992) Effects of buprenorphine on self-administration of cocaine and a nondrug reinforcer in rats. Psychopharmacology (Berl) 106:439–446.

Cole SL, Robinson MJ, Berridge KC (2018) Optogenetic self-stimulation in the nucleus accumbens: D1 reward vs D2 ambivalence. PLoS One 13: e0207694.

Corre J, van Zessen R, Loureiro M, Patriarchi T, Tian L, Pascoli V, Lüscher C (2018) Dopamine neurons projecting to medial shell of the nucleus accumbens drive heroin reinforcement. Elife 7:e39945.

Creed M, Kaufling J, Fois GR, Jalabert M, Yuan T, Lüscher C, Georges F, Bellone C (2016) Cocaine exposure enhances the activity of ventral tegmental area dopamine neurons via calcium-impermeable NMDARs. J Neurosci 36:10759–10768.

Crummy EA, O'Neal TJ, Baskin BM, Ferguson SM (2020) One is not enough: understanding and modeling polysubstance use. Front Neurosci 14:569.

Dobbs LK, Kaplan AR, Lemos JC, Matsui A, Rubinstein M, Alvarez VA (2016) Dopamine regulation of lateral inhibition between striatal neurons gates the stimulant actions of cocaine. Neuron 90:1100–1113.

Duarte M, Watanabe RN (2021) Notes on scientific computing for biomechanics and motor control (version 0.0.2). Zenodo.

Everitt BJ, Giuliano C, Belin D (2018) Addictive behaviour in experimental animals: prospects for translation. Philos Trans R Soc Lond B Biol Sci 373:20170027.

Ferguson SM, Eskenazi D, Ishikawa M, Wanat MJ, Phillips PE, Dong Y, Roth BL, Neumaier JF (2011) Transient neuronal inhibition reveals opposing roles of indirect and direct pathways in sensitization. Nat Neurosci 14:22–24.

Gerfen CR, Surmeier DJ (2011) Modulation of striatal projection systems by dopamine. Annu Rev Neurosci 34:441–466.

Grimm JW, Hope BT, Wise RA, Shaham Y (2001) Incubation of cocaine craving after withdrawal. Nature 412:141–142.

Hedegaard H, Miniño AM, Warner M (2018) Drug overdose deaths in the United States, 1999-2017. NCHS Data Brief.

Isaacs DP, Leman RP, Everett TJ, Lopez-Beltran H, Hamilton LR, Oleson EB (2020) Buprenorphine is a weak dopamine releaser relative to heroin, but its pretreatment attenuates heroin-evoked dopamine release in rats. Neuropsychopharmacol Rep 40:355–364.

Johnson SW, North RA (1992) Opioids excite dopamine neurons by hyperpolarization of local interneurons. J Neurosci 12:483–488.

Koob GF, Volkow ND (2016) Neurobiology of addiction: a neurocircuitry analysis. Lancet Psychiatry 3:760–773.

Kremer EJ, Boutin S, Chillon M, Danos O (2000) Canine adenovirus vectors: an alternative for adenovirus-mediated gene transfer. J Virol 74:505–512.

Kupchik YM, Brown RM, Heinsbroek JA, Lobo MK, Schwartz DJ, Kalivas PW (2015) Coding the direct/indirect pathways by D1 and D2 receptors is not valid for accumbens projections. Nat Neurosci 18:1230–1232.

Lerner TN, Shilyansky C, Davidson TJ, Evans KE, Beier KT, Zalocusky KA, Crow AK, Malenka RC, Luo L, Tomer R, Deisseroth K (2015) Intact-brain analyses reveal distinct information carried by SNc dopamine subcircuits. Cell 162:635–647.

Lobo MK, Covington HE, Chaudhury D, Friedman AK, Sun H, Damez-Werno D, Dietz DM, Zaman S, Koo JW, Kennedy PJ, Mouzon E, Mogri M, Neve RL, Deisseroth K, Han MH, Nestler EJ (2010) Cell type-specific loss of BDNF signaling mimics optogenetic control of cocaine reward. Science 330:385–390.

Löw K, Aebischer P, Schneider BL (2013) Direct and retrograde transduction of nigral neurons with AAV6, 8, and 9 and intraneuronal persistence of viral particles. Hum Gene Ther 24:613–629.

Luo Z, Volkow ND, Heintz N, Pan Y, Du C (2011) Acute cocaine induces fast activation of D1 receptor and progressive deactivation of D2 receptor striatal neurons: in vivo optical microprobe $[Ca^{2+}]_i$ imaging. J Neurosci 31:13180–13190.

Maldonado R, Saiardi A, Valverde O, Samad TA, Roques BP, Borrelli E (1997) Absence of opiate, rewarding effects in mice lacking dopamine D2 receptors. Nature 388:586–589.

Martianova E, Aronson S, Proulx CD (2019) Multi-fiber photometry to record neural activity in freely-moving animals. J Vis Exp 152:e60278.

Masamizu Y, Okada T, Kawasaki K, Ishibashi H, Yuasa S, Takeda S, Hasegawa I, Nakahara K (2011) Local and retrograde gene transfer into primate neuronal pathways via adeno-associated virus serotype 8 and 9. Neuroscience 193:249–258.

Meng C, Zhou J, Papaneri A, Peddada T, Xu K, Cui G (2018) Spectrally resolved fiber photometry for multi-component analysis of brain circuits. Neuron 98:707–717.e4.

O'Neal TJ, Nooney MN, Thien K, Ferguson SM (2020) Chemogenetic modulation of accumbens direct or indirect pathways bidirectionally alters reinstatement of heroin-seeking in high- but not low-risk rats. Neuropsychopharmacology 45:1251–1262.

Park K, Volkow ND, Pan Y, Du C (2013) Chronic cocaine dampens dopamine signaling during cocaine intoxication and unbalances D1 over D2 receptor signaling. J Neurosci 33:15827–15836.

Patriarchi T, Cho JR, Merten K, Howe MW, Marley A, Xiong WH, Folk RW, Broussard GJ, Liang R, Jang MJ, Zhong H, Dombeck D, von Zastrow M, Nimmerjahn A, Gradinaru V, Williams JT, Tian L (2018) Ultrafast neuronal imaging of dopamine dynamics with designed genetically encoded sensors. Science 360:eaat4422.

Patriarchi T, Mohebi A, Sun J, Marley A, Liang R, Dong C, Puhger K, Mizuno GO, Davis CM, Wiltgen B, von Zastrow M, Berke JD, Tian L (2020) An expanded palette of dopamine sensors for multiplex imaging in vivo. Nat Methods 17:1147–1155.

Paxinos G, Watson CR, Emson PC (1980) AChE-stained horizontal sections of the rat brain in stereotaxic coordinates. J Neurosci Methods 3:129–149.

Phillips PE, Stuber GD, Heien ML, Wightman RM, Carelli RM (2003) Subsecond dopamine release promotes cocaine seeking. Nature 422:614–618.

Plotkin JL, Shen W, Rafalovich I, Sebel LE, Day M, Savio Chan C (2013) Regulation of dendritic calcium release in striatal spiny projection neurons. J. Neurophysiol 110:2325–2336.

Sellings LH, Clarke PB (2003) Segregation of amphetamine reward and locomotor stimulation between nucleus accumbens medial shell and core. J Neurosci 23:6295–6303.

Shaham Y, Shalev U, Lu L, De Wit H, Stewart J (2003) The reinstatement model of drug relapse: history, methodology and major findings. Psychopharmacology (Berl) 168:3–20.

Shippenberg TS, Bals-Kubik R, Herz A (1993) Examination of the neurochemical substrates mediating the motivational effects of opioids: role of the mesolimbic dopamine system and D-1 vs. D-2 dopamine receptors. J Pharmacol Exp Ther 265:53–59.

Siciliano CA, Tye KM (2019) Leveraging calcium imaging to illuminate circuit dysfunction in addiction. Alcohol 74:47–63.

Soares-Cunha C, Coimbra B, David-Pereira A, Borges S, Pinto L, Costa P, Sousa N, Rodrigues AJ (2016) Activation of D2 dopamine receptor-expressing neurons in the nucleus accumbens increases motivation. Nat Commun 23:11829.

Soares-Cunha C, de Vasconcelos NA, Coimbra B, Domingues AV, Silva JM, Loureiro-Campos E, Gaspar R, Sotiropoulos I, Sousa N, Rodrigues AJ (2019) Nucleus accumbens medium spiny neurons subtypes signal both reward and aversion. Mol Psychiatry 25:3241–3255.

Stinus L, Nadaud D, Deminière JM, Jauregui J, Hand TT, Le Moal M (1989) Chronic flupentixol treatment potentiates the reinforcing properties of systemic heroin administration. Biol Psychiatry 26:363–371.

Swapna I, Bondy B, Morikawa H (2016) Differential dopamine regulation of $Ca^{2+}$ signaling and its timing dependence in the nucleus accumbens. Cell Rep 15:563–573.

Taverna S, Ilijic E, Surmeier DJ (2008) Recurrent collateral connections of striatal medium spiny neurons are disrupted in models of Parkinson's disease. J Neurosci 28:5504–5512.

Tervo DG, Hwang BY, Viswanathan S, Gaj T, Lavzin M, Ritola KD, Lindo S, Michael S, Kuleshova E, Ojala D, Huang CC, Gerfen CR, Schiller J, Dudman JT, Hantman AW, Looger LL, Schaffer DV, Karpova AY (2016) A designer AAV variant permits efficient retrograde access to projection neurons. Neuron 92:372–382.